Author version: *Environ. Monit. Assess., vol.187(11); 2015; no.675 doi: 10.1007/s10661-015-4870-2*

Residual fluxes of water and nutrient transport through the main inlet of a tropical estuary, Cochin estuary, West Coast, India

Revichandran C., Vinita J., Lallu K.R., Muraleedharan K. R., Jineesh V.K., Shivaprasad A.

Abstract

Determining robust values for estuarine material fluxes has been a complex task and an interdisciplinary research challenge. With the advent of Acoustic Doppler Profilers (ADPs) having bottom-track capability and which provides three-dimensional current velocity profiles, more accurate estimation of cross sectional fluxes is far accomplished in unsteady and bi-directional flow conditions of estuaries. This paper reports for the first time the discharge measurements conducted across Cochin inlet using ADP to examine the spring-neap variability in residual fluxes of water and nutrients during dry season. Cross sectional current velocity profiles and salinity profiles were captured using ADP and CTD. Samples of surface and bottom water were also collected at three hour intervals. The results indicated that there is a distinct transition from the neap to spring tides related to flow and salinity structure. The neap tide was partially mixed with large diurnal inequalities whereas the spring tide was well-mixed with symmetric tides. During ebb, an increase in the concentrations of nitrate, nitrite, phosphate and silicate was noticed indicating upstream sources for their inputs. In contrast, elevated levels of ammonia were found in the estuary throughout the period of observation. There was net residual outflow during both tides and the computed residual water fluxes of neap doubled that of spring. The strong ebb currents and the increased nutrient concentrations during ebb resulted in the export of all nutrients (except ammonia during spring) into the sea. The findings of this study highlight the consequences of anthropogenic interventions in the estuary and their effects on the fluxes of ecologically relevant substances.

Key words: residual; fluxes; nutrients; diurnal; Acoustic Doppler Profiler; Cochin inlet

1. Introduction

Interactions across the land-ocean boundary are currently the focus of regional and global research to quantify fluxes of materials from the land to the coastal region which determines the anthropogenic effects on the coastal environment. The concentration of land-ocean fluxes in estuaries apparently offers the prospect of estimating net transport to the ocean from the upstream estuarine sections. Quantification of these fluxes is an important objective in the evaluation of environmental impacts (Lane et al. 1997). The determination of net fluxes in estuaries is, however, complicated by tidal motions which require observations to be extensive in time, in order to allow averaging over tidal cycles, and of sufficient spatial resolution to permit accurate integration across the estuary section. Direct determination of net flux at a cross section has a long and generally discouraging history in estuarine oceanography (Jay et al. 1997). The development of Acoustic Doppler Profiler (ADP) and its application to estuaries offers a potential to decrease the time required in data acquisition and to provide data of greater spatial resolution than traditional methods. In addition, ADPs provide a continuous data collection throughout the water column and cross section rather than discrete point measurements.

Cochin estuary is the second largest estuary along west coast of India. However, reclamations over the past several decades have resulted in considerable shrinkage (40%) of the estuary (Gopalan et al. 1983). The ongoing dredging associated with port development and maintenance has deepened and widened the lower estuarine reaches which can change the tidal range, tidal prism, ebb and flood tide velocities and can also cause bank instability. In addition, increased anthropogenic activities from the mid 1970s have seriously polluted the estuary by industrial discharges (Balachandran et al. 2005). Eutrophication caused by the excess supply of anthropogenic nutrients has become a major threat for the ecosystem functioning (Madhu et al. 2007, Martin et al. 2011, Martin et al. 2013, Rajaneesh et al. 2015). Heavy metal pollution in the estuary has increased significantly through the discharge of industrial and domestic wastes (Nair and Sujatha 2013) which can adversely affect the estuarine microbial diversity (Jose et al. 2011) and benthic organisms (Martin et al. 2012). Increased human activities has sustained a very high population of virus and bacteria in the estuary (Parvathi et al. 2015).

In the recent years, numerous studies have been carried out to examine the dynamics of Cochin estuary. Revichandran et al. (2011) reported that the amplitude of water level decreased to a minimum in the central area between the two inlets in the northern arm of the estuary. The variations in stratification due to runoff or due to the closure of an artificial barrage situated upstream influenced the distribution of chemical and biological parameters within the estuary (Shivaprasad et al. 2013a, 2013b). The flushing time scales of the estuary ranged from 1 to 2.5 days during the wet season and were 8.7 days during the dry season (Vinita et al. 2015a). The high flushing rates caused by river runoff had direct influence on

nutrient transport (Lallu et al. 2014) and plankton dynamics (Sooria et al. 2015) of the estuary. In addition, tides in the estuary are mixed and predominantly semidiurnal in nature thereby inducing significant spatial changes in flood-ebb asymmetries (Vinita et al. in press). Although these studies reveal the hydrodynamics and the environmental status of the estuary, efforts to measure the residual fluxes is limited due to the lack of high resolution data. Lallu et al. (2014) had attempted to quantify the net material fluxes using current meter records at multiple stations during October 2009. In their study, the current profiles at the Cochin inlet station was obtained by single-point sampling using two current meters positioned at the surface and bottom. However, discharge estimates using conventional mechanical current meters often yielded great errors (Simpson and Bland 2000). Realizing the difficulty to accurately measure fluxes via single point current meter records, ADPs were introduced in Cochin estuary for the first time in the year 2010. In addition, unlike the previous studies which focused mainly on the influence of river runoff and the high flushing rates on the fluxes and environmental conditions of Cochin estuary, the present study was conducted during dry season (February and March 2010) when tidal actions are predominant. Series of moving boat ADP discharge measurements were conducted across Cochin inlet under neap and spring tidal cycles to quantify the residual fluxes of water. Simultaneous nutrient concentrations were also determined to estimate the net nutrient transport through Cochin inlet.

2. Materials and methods

2.1 Environmental set up

Cochin estuary extends from Munambam (10°10'N, 76°15' E) in the north, to Thannermukkam (09°30' N, 76°25' E) in the south over a length of ~80 km covering an area of about 300 km^2 (Figure 1). The system is characterized by its long axis lying parallel to the coastline connecting the sea at two inlets: Munambam and Cochin. Cochin inlet is relatively wider and deeper. The widths and depths from mouth (Cochin inlet) to head (Thanneermukkam) range from 450m to 4km and 15m to 3m respectively. The freshwater runoff into the estuary is primarily contributed by rivers Periyar, Pampa, Achankovil, Manimala, Meenachil and Muvattupuzha. The river runoff is high during wet season (June-September) characterized by Indian Summer Monsoon (ISM). This period is followed by a moderate runoff period (October-December) and the rest of the year represents the peak dry season. The monthly mean river runoff obtained from Central Water Commission for the year 2010 is presented in Figure 2. It varies from 158m^3s^{-1} in February to 1463m^3s^{-1} in July. The estuary undergoes a transition from salt wedge type during wet season to a completely well-mixed state during the peak dry season (Shivaprasad et al. 2013a). While Cochin inlet is ebb dominant, the main channel areas are flood dominant in nature during dry season (Vinita et al. in press).

2.2 Data collection and analysis

A 24h field experiment was carried out at Cochin inlet for two consecutive tidal cycles of neap (22-23 February 2010) and spring (1-2 March 2010) tides of dry season. These months were selected for this intensive survey including physical and chemical parameters to minimize the likelihood of major non-tidal current components (river runoff). Water level was recorded at 10 minute intervals using SBE 26 plus Tide Recorder with accuracy 0.1% of full scale (Strain Gauge Pressure) which was installed at the estuarine margins near to the sampling cross sections. Current velocity and total cross section discharge were acquired using ADP with bottom track capability. A Sontek ADP (1500 kHz) was towed 450m across the inlet for every 3h which acquired vertical velocity (± 1 % accuracy) profiles at 5s averaging rate and 0.9m of vertical resolution (cell size). The cross-channel transects were undertaken from right bank to left bank (Figure 1). The boat speed (from bottom-track data) was subtracted from the measured water velocity to give absolute current profile independent of boat motion. Downstream currents are assigned positive and upstream currents are assigned negative. The discharge computations were made using the proprietary software Sontek's RiverSurveyor. A sixth order polynomial was fitted (R^2=0.9) to the relation between water level and ADP discharge to derive hourly flux values.

Salinity profiles were taken using SBE Seabird 19 plus CTD (conductivity ± 0.001 Sm−1) with a bin size 0.2 m for every 1h interval at the middle of the transect (depth of 10m) (Figure 1). Current profile at this CTD sampling station was extracted from the ADP cross-channel data to examine the evolution of currents and stratification over tidal cycles. Using this data, the gradient Richardson number (*Ri*), which provides stability of the water column were computed at 3h interval from equation,

$$Ri = \frac{g\partial\rho/\partial z}{\rho\left(\frac{\partial u}{\partial z}\right)^2} \qquad \text{---------- (1)}$$

where ρ is the mean density, $\partial\rho/\partial z$ is the mean vertical density gradient, g is the gravitation acceleration and $\partial u/\partial z$ is the mean vertical shear. When stratification is of more importance than mixing, *Ri* is greater than 0.25. When *Ri* values are lower than 0.25, mixing prevails as a result of shear instability (Miles 1961).

At the same location, water samples were also collected from 0.5 m below the surface and 0.5 m above the bottom at 3h intervals using 5L Niskin sampler (Hydro-Bios, Kiel-Holtenau, Germany) simultaneous with the ADP discharge measurement for both tides. The samples for dissolved oxygen (DO) collected without air bubbles in glass bottles were fixed onboard and later analyzed according to Winkler's method (Grasshoff et al. 1983). The water samples for the determination of various dissolved inorganic nutrients were collected in 500ml PVC bottles, kept in ice boxes and filtered through

Whatman no.1 filter paper (pore size 1 μm) in the laboratory at the earliest possible time. Nitrite-N was determined through the formation of a reddish purple azo dye following the method of Bendschneider and Robinson (1952). Nitrate-N was measured by reduction to nitrite in a copper-cadmium reduction column (APHA 2000). Ammonia-N and silicate- Si were estimated by phenate method (APHA 2000) and by ascorbic acid method (Koroleff 1983) respectively. Phosphate- P was measured using ascorbic acid as reducing agent (APHA, 2000). All the dissolved nutrients were analyzed using a UV-VIS Spectrophotometer (Shimadzu 1650PC) calibrated with respective standard solutions. Nutrient transport at the inlet during consecutive neap and spring tides was computed with the instantaneous discharge values (m^3s^{-1}) obtained from ADP measurements multiplied by the corresponding nutrient concentration (μM converted to kgm^{-3}). Net fluxes are represented in tons per day (t d^{-1}). The export fluxes were symbolized as positive and import fluxes as negative with respect to downstream and upstream currents.

3. Results

3.1 Time series of water level, currents and salinity

Variations in water level, currents and stratification for neap and spring tides are summarized in the Figure 3. Figures 3a and 3b demonstrate that tidal cycles were mixed semi-diurnal for both tidal phases with diurnal inequality. The maximum tidal range for neap tide was 75.4cm (Figure 3a) which increased to 93.9cm for spring tide (Figure 3b). Pronounced diurnal inequality was observed for neap with the largest occurring during low tides (36.9cm). The difference between high tides during neap, however, decreased to 4.9cm.The diurnal inequality at spring tide was 6.4cm and 15.1cm for low and high tides respectively. The currents were vertically homogeneous and were unidirectional for both tides (Figures 3c, 3d). The neap observations indicated that the current peaks were 150cm s^{-1} with a direction of 246° (with respect to true north) during ebb and were -125 cm s^{-1} with a direction of 84° during flood periods (Figure 3c). The highest ebb velocity occurred at the surface while the highest flood velocity occurred at the bottom. During spring tide, the maximum flood was -162 cm s^{-1} toward 76° and maximum ebb was 131 cm s^{-1} toward 262° (Figure 3d). The highest flood and ebb velocities were found at the surface.

A phase lag between water level and salinity was more pronounced for neap (Figures 3a, 3e) than spring tide (Figures 3b, 3f). The salinity field under neap tides showed a definite stratification feature, with fresher water of 21.7 at the upper layer and saltier water of 30·6 at the bottom during the initial ebb ($Ri \sim 0.9$) (Figure 3e). After slack, stratification gradually declined and near lowest high water (LHW), the water column was homogeneous with salinity of about 31 psu ($Ri<0.25$). Similar observations were found in the following tidal cycle also but with relatively lower stratification during

ebb (*Ri* ~ 0.7) and mixing at highest high water (HHW) (*Ri* ~ 0.4). During spring tide, the salinity gradients between surface and bottom was lower (~5.3) compared to neap tide (~8.9) (Figure 3f). Although slighter stratification was developed during low water, the highly turbulent tidal flood currents mixed the whole water column, raising salinity to 33 psu. *Ri* values were less than 0.25 throughout the observation period with the least value of 0.02 found during HHW indicating turbulence which is largely unaffected by stratification.

3.2 Cross-channel currents and residual water fluxes

Typical cross-channel current speed and direction contour plots for neap and spring tides measured using ADP are shown in the Figure 4. During neap, the maximum cross-sectional mean velocity of 98 cm s^{-1} occurred at 9:00h (Julian day 53.38) (Figure 4a) close to lowest low water (LLW) (Figure 3a). The dominant direction of the current profiles were also seaward (270°) during that time (Figure 4a). In the landward direction (90°), the maximum mean velocity of 68 cm s^{-1} was attained at 18:00 h (Julian day 53.75) (Figure 4b) close to LHW (Figure 3a). During spring, the currents peaked to 84 cm s^{-1} in the landward direction at 0:00h (Julian day 61) at HHW (Figure 4c, 3b) whereas maximum mean velocity of 96 cm s^{-1} in the seaward direction occurred at 6:00 h (Julian day 61.27) close to LLW (Figure 4d, 3b).

Figure 5 shows the relation of water flux variability for neap and spring tides with the observed water level. During neap tide, the maximum seaward flux occurred close to lowest low water (LLW) reaching 5305 m^3s^{-1} (Figure 6a). The first high water took place about 8 h after low water, increasing the landward flux to a maximum value of 2807 m^3s^{-1} near LHW. Then, highest low water (HLW) occurred soon after 4h which reduced the instantaneous flux to near zero values. Under spring tidal conditions, the landward fluxes began to increase about 2h after HLW, reaching 5193.7 m^3s^{-1} near HHW (Figure 6b). The ebb flow commenced approximately 3h after HHW, giving an outward water transport peak of 5381.8 m^3s^{-1} at the 22^{nd} hour of the tidal cycle near LLW. There is a phase lag between the calculated fluxes and water level for both tides; about 4.5 h in neap and about 2.5 h in spring. While the spring-neap variability in the maximum seaward fluxes was low (neap: 5305.3 m^3s^{-1}; spring: 5381.8 m^3s^{-1}), large differences were exhibited for maximum landward fluxes (neap: 3006.6 m^3s^{-1}; spring: 5193.7 m^3s^{-1}). The residual fluxes of water over the tidal cycles were 4990.8 m^3s^{-1} and 2149.7 m^3s^{-1} for neap and spring tides respectively, directed seaward during both tidal phases.

3.3 Nutrient distribution and net transport

The mean DO values for neap and spring tides were 5.32±0.4 mg/L and 4.48± 0.6 mg/L respectively. The minimal range (2.98-5.82 mg/L) in oxygen concentration occurred in spring tide. The

tidally averaged surface values of all nutrients, other than NH_4 were higher during neap than spring tide (Figure 6a). At the bottom, PO_4 and SiO_4 concentrations were comparatively higher during spring suggesting that enhanced turbulence due to strong currents facilitated the release of substances from bottom sediments (Figure 6b). The difference between surface and bottom nutrients (except NH_4) was larger during neap than spring tides owing to the observed stratification during neap tide. Distinctly, the surface mean values of NH_4 during spring (23 μM) were higher than neap (17 μM) whereas the bottom mean values (~16μM) were similar for both tidal phases. The maximal surface-bottom variability (neap: 15.7μM; spring: 9.2 μM) was observed for SiO_4 irrespective of the tidal phases. The predominant form of dissolved inorganic nitrogen (DIN) was NH_4, constituting 55% and 75% during neap and spring tides respectively, followed by NO_3 and NO_2. The tidally averaged values of N/P ratio were higher for neap (43:1) than spring (28:1) owing to increased NO_3 concentration. Pearson correlation matrix of salinity and nutrients for neap and spring tides are presented in Table 1. Concentration of NO_2, PO_4 and SiO_4 displayed strong inverse relationship with salinity (R^2=0.96) for neap and spring tides. NO_3 was negatively correlated ($p<0.001$) with salinity during spring whereas, for neap the relation was poor due to its large variability. No significant relation was found between NH_4 and salinity. From these statistical analyses, it is presumed that sources of NO_2, PO_4 and SiO_4 were mainly riverine, while there exists several nonpoint sources for NO_3 and NH_4.

The pronounced intra-tidal and spring-neap variations in nutrient distribution were also reflected in the net transport of nutrients through the Cochin inlet (Table 2). The computed net fluxes were positive for all nutrients irrespective of the tidal phases except NH_4 on spring tide. The maximum net fluxes were obtained for NH_4 which showed positive (245.68t/d) and negative (132.93t/d) values for neap and spring tides respectively. Evidently, there was a decrease in the net fluxes of all nutrients during spring compared to neap tides. NO_3 fluxes decreased from 81.13t/d on neap to 2.51t/d on spring tides. The DIN fluxes were also calculated which showed a net export of 331t/d during neap while a net import of 128t/d during spring tides.

4. Discussion

The material transport in estuaries is affected by diurnal inequality and its rate varies over spring-neap cycles and seasonal scales (Uncles and Jordan 1979). The present study during the tidally dominated period (dry season) showed that the neaps were characterized by strong diurnal inequality, while the spring tides were more symmetric. These tidal characteristics directly influenced the stratification and residual fluxes through the main inlet. Shivaprasad et al. (2013a) had reported the occurrence of a similar diurnal inequality during neap tide of wet season which controls the advancement of salt wedge at high tides and retreat during low tides.

The currents structure and salinity illustrate the dynamic nature of the flows with tidal time-scale variations at the site (Figure 3). A transition from partially mixed neap tide to well mixed spring tide was observed during dry season. The role of diurnal inequality in setting the pattern of currents and salinity was discernible. In neap tide, for the first tidal cycle, the initial ebb was strong with current speeds ranging from 8cm s^{-1} to 150cm s^{-1} (Figures 3a and 3c). The subsequent flood took about 8 h to reach the LHW with velocities ranging from 14 cm s^{-1} to 125 cm s^{-1}. This was followed by a shorter (4 h) but slower (~26 cm s^{-1}) ebb period. Due to the large tidal prism (change in volume of water between high tide and low tide) of the first tidal cycle, the current speeds during second flood leading to HHW was weak ~ 23cm s^{-1} (Figure 3c). Higher and prolonged stratification was also found during the initial ebb compared to the following ebb tide which can be attributed to the large inequality in the low tide ranges (Figure 3e). On the other hand, spring tides were almost symmetric and the current strength, stratification and fluxes corresponded well with the water level changes. Strongest currents and intense turbulent mixing period with vertical isohalines were observed during the highest tides (HHW) (Figures 3b and 3d). The range of variability in the salinity was reduced during the spring due to a reduction in the diurnal inequality (Figure 3f).

The cross-channel ADP measurements showed that the peak ebb currents that occurred for both tides were similar in magnitude (~ 100 cm s^{-1}) but peak flood currents of neap were lower than spring by about 20 cm s^{-1} (Figures 4). These intra-tidal and spring-neap variations in current speeds were also reflected in the residual fluxes of water. The maximum seaward fluxes for spring and neap tides were similar whereas the spring landward fluxes were higher (Figure 5). The observed stronger ebb than flood currents implied residual outflow on the neap and spring tides. Moreover, for neap tide the computed residual fluxes were almost double that of spring tide. Tidal forcing downstream reduces the seaward fluxes and the effect becomes prominent during spring tides when the tidal ranges are higher (Godin 1988). Diurnal inequality played a prominent role in neap tide as the maximum landward fluxes occurred close to LHW, unlike spring tide, where the maximum fluxes coincided with HHW.

The direct impact of the hydrodynamics on the nutrient distributions at Cochin inlet was also assessed. The highest concentration of nutrients in the region was associated with waters of upstream origin and lower salinities. The strong inverse relationship of SiO_4, PO_4, and NO_2 with salinity for spring and neap tides indicated freshwater as their main source of inputs. However, NH_4 and NO_3 concentrations did not show significant relationship with salinity due to their possible supply from nonpoint sources like urban and industrial discharges (Martin et al. 2013, Bhavya et al. 2015). In addition, NH_4 and NO_3 concentrations in the estuary are often controlled by the processes such as organic matter decomposition, nitrification and nitrogen fixation apart from sediment re-suspension (Miranda et al. 2008, Vipindas et al. 2015). Bhavya et al. (2015) pointed out that despite the high

nitrification rates and biological assimilation prevailing in Cochin estuary, the ammonia pollution is only moderately reduced. During ebb tide an increase in SiO_4, PO_4, NO_2 and NO_3 in the water column was noticed. The stronger ebb currents and increased ebb nutrient concentration resulted in the export of all nutrients (except ammonia during spring) into the sea (Table 2). The decrease in the nutrient fluxes during spring could be attributable to the relatively lower nutrient concentration and the reduction in the residual outflow. In a recent study during post monsoon season (September–October 2009) by Lallu et al. (2014), Cochin estuary was reported to be a matured system, since it exported substantial amount of nutrients.

Negative NH_4 fluxes during spring tide were due to its higher concentration during flood. NH_4 could be imported from the coastal waters where the organic matter remineralisation processes may regenerate nutrients in the sediment (Dunn et al. 2008). In the western Indian inner shelf regions, the nutrient demands for phytoplankton production is supplied by benthic regeneration during dry season (February–March) (Naqvi et al. 2006) and a maximum benthic release of NH_4 (>50%) is observed (Prathihary et al. 2014). The stronger coastal currents during spring can cause nutrient diffusion in the water column which is likely to advect to the estuary with the incoming flood tide.

Table 2 presents the nutrient fluxes measured during dry season in other Indian estuarine systems for comparison. It should be noted that while Cochin estuary and Hoogly estuary generally showed large seaward fluxes of nutrients, the fluxes of Chaliyar estuary and Tapi estuary were smaller and directed landward. Although the fluxes of DIN from Cochin estuary were larger compared to the estimates of Hoogly estuary, the phosphate and silicate fluxes were more or less similar. The greater export fluxes from Cochin estuary to the coastal water indicated excessive nutrient supply from nonpoint sources like municipal and industrial waste discharges during dry season.

5. Conclusion

The results of the present study showed that at Cochin inlet during dry season, strong diurnal inequality was present for neap tide whereas spring tide was almost symmetric. Due to stronger ebb currents, the net residual fluxes were directed seaward and for neap tide the fluxes were almost double that of spring tide. The study also provides more reliable estimates of nutrient fluxes through the inlet by means of ADP measurements during dry season. Despite the low runoff conditions during dry season, generally a net export of materials through Cochin inlet was observed. This was due to the characteristic ebb dominance of tidal currents compounded with the increased ebb concentrations of nutrients. The vast export of nutrients from the estuary has direct impact on the coastal productivity which is substantiated by the frequent occurrences of blooms in the adjacent coastal areas, even during dry season

(D'silva et al. 2012). The study highlights the need for future interdisciplinary research utilizing simultaneous ADP measurements across river mouths and inlets for different seasons to quantify the material inputs and outputs.

6. Acknowledgement

Authors are thankful to the Director, CSIR-NIO and Scientist In-Charge, Regional Centre, Kochi for their keen encouragement and support. The study forms a part of the project "Ecosystem modeling of Cochin backwaters" funded by Integrated Coastal and Marine Area Management (ICMAM-PD), Ministry of Earth Sciences, Chennai. We extend our thanks to the staff and research students of NIO for their valuable assistance during field collections. This paper work is a part of the doctoral research of the author, Vinita J. who acknowledges the Council of Scientific and Industrial Research, New Delhi, for the financial support in the form of senior research fellowship. This is NIO Contribution No. xxxx.

7. Compliance with Ethical Standards

The authors declare that they have no conflict of interest.

This article does not contain any studies with human participants or animals performed by any of the authors.

Informed consent was obtained from all individual participants included in the study.

8. References

APHA 2000. *Standard Methods for the Examination of Water and Wastewater*. 21sted. Eaton, A. D., Clesceri, L. C., Greenberg, A. E., et al. (Eds.), Washington, DC: American Public Health Association.

Balachandran, K.K., Laluraj, C.M., Nair, M., Joseph, T., Sheeba, P., et al. (2005). Heavy metal accumulation in a flow restricted tropical estuary. *Estuarine, Coastal and Shelf Science*, *65*, 361 – 370.

Bapardekar, M. V., de Sousa, S. N., Zingde, M. D., et al. (2004). Biogeochemical Budgets for Tapi Estuary. In Final Report for APN Project: An Assessment of Nutrient, Sediment and Carbon Fluxes to the Coastal Zone in South Asia and their Relationship to Human Activities (pp. 359) Sri Lanka National Committee of IGBP; Sri Lanka Association for the Advancement of Science.

Bendschneider, K., & Robinson, R. (1952). A new spectrophotometric method for the determination of nitrite in sea water. *Journal of Marine Research*, *11*(1), 87-96.

Bhavya, P. S., Kumar, S., Gupta, G. V. M., Sudheesh, V., Sudharma, K. V., Varrier , D. S., Dhanya K. R., Saravanane, N., et al. (2015). Nitrogen Uptake Dynamics in a Tropical Eutrophic Estuary (Cochin, India) and Adjacent Coastal Waters. *Estuaries and Coasts,* doi: 10.1007/s12237-015-9982-y

D'Silva, M. S., Anil, A. C., Naik, R. K., D'Costa, P. M., et al. (2012). Algal blooms: a perspective from the coasts of India. *Natural Hazards, 63*(2), 1225–1253, doi:10.1007/s11069-012-0190-9

Dunn, R. J. K., Welsh, D. T., Teasdale, P. R., Lee, S. Y., Lemckert, C. J., Meziane, T., et al. (2008). Investigating the distribution and sources of organic matter in surface sediment of Coombabah Lake (Australia) using elemental, isotopic and fatty acid biomarkers. *Continental Shelf Research, 28*(18), 2535–2549, doi:10.1016/j.csr.2008.04.009

Godin, G. 1988. *Tides*. Anadyomene Edition, Ottawa, Ontario, Canada.

Gopalan, U.K., Vengayil, D.T., Udaya Varma, P., Krishnankutty, M., et al. (1983). The shrinking backwaters of Kerala. *Journal of Marine Biological Association of India, 25*, 131–141.

Grasshoff, K., Ehrhardt, M., Kremling, K., et al. (1983). *Methods of seawater analysis*. (2nd Ed.), Weinheim: Deerfield Beach, Florida Basel, Verlagchemie.

Jay, D., Uncles, R., Largier, J., Geyer, W.R., Vallino, J., Boynton, W., et al. (1997). A review of recent developments in estuarine scalar flux estimation. *Estuaries, 20*, 262-280.

Jose, J., Giridhar, R., Anas, A., LokaBharati, P.A., Nair, S., et al. (2011). Heavy metal pollution exerts reduction/adaptation in the diversity and enzyme expression profile of heterotrophic bacteria in Cochin estuary, India. *Environmental Pollution, 159,* 2775-2780.

Koroleff, F. (1983). Determination of silicon. In Grasshoff, K., Ehrhardt, M., Kremling, K. (Eds.), Methods of seawater analysis: second, revised and extended edition (pp. 174-183). Weinheim: VerlagChemie.

Lallu, K. R., Fausia, K. H., Vinita, J., Balachandran, K. K., Naveen Kumar, K. R., et al. (2014) Transport of dissolved nutrients and chlorophyll a in a tropical estuary, southwest coast of India. *Environmental Monitoring and Assessment*, doi: 10.1007/s10661-014-3741-6

Lane, A., Prandle, D., Harrison, A. J., Jones, P. D., Jarvis, C. J., et al. (1997). Measuring fluxes in tidal estuaries: Sensitivity to instrumentation and associated data analyses. *Estuarine, Coastal and Shelf Science, 45*, 433-451.

Madhu, N., Jyothibabu, R., Balachandran, K., Honey, U., Martin, G., Vijay, J., Shiyas, C., Gupta, G., Achuthankutty, C., et al. (2007). Monsoonal impact on planktonic standing stock and abundance in a tropical estuary (Cochin backwaters—India). *Estuarine, Coastal and Shelf Science, 73*, 54–64.

Martin, G., Nisha, P., Balachandran, K., Madhu, N., Nair, M., Shaiju, P., Joseph, T., Srinivas, K., Gupta, G., et al. (2011). Eutrophication induced changes in benthic community structure of a flow-restricted tropical estuary (Cochin backwaters), India. *Environmental Monitoring and Assessment*, *176*, 427–438.

Martin, G., George, R., Shaiju, P., Muraleedharan, K., Nair, S., Chandramohanakumar, N., et al. (2012). Toxic metals enrichment in the surficial sediments of a eutrophic tropical estuary (Cochin Backwaters Southwest coast of India). *The Scientific World Journal*, doi: 10.1100/2012/972839.

Martin, G. D., Jyothibabu, R., Madhu, N. V, Balachandran, K. K., Nair, M., & Muraleedharan, K. R., et al. (2013). Impact of eutrophication on the occurrence of Trichodesmium in the Cochin backwaters, the largest estuary along the west coast of India, *Environmental Monitoring and Assessment, 185*(3), 1–28.

Miles, J. (1961). On the stability of heterogeneous shear flows. *Journal of Fluid Mechanics*, *10,* 496–508.

Miranda, J., Balachandran, K. K., Ramesh, R., Wafar, M., et al. (2008). Nitrification in Kochi backwaters. *Estuarine, Coastal and Shelf Science*, *78*, 291-300.

Mukhopadhyay, S. K., Biswas, H., De, T. K., Jana, T. K. (2006). Fluxes of nutrients from the tropical River Hooghly at the land–ocean boundary of Sundarbans, NE Coast of Bay of Bengal, India. *Journal of Marine Systems, 62*, 9-21.

Nair, M. P. & Sujatha, C. H. (2013). Environmental Geochemistry of Core Sediment in the Cochin Estuary (CE), India. *Research Journal of Chemical Sciences, 3*(4), 65-69.

Naqvi, S. W. A., Naik, H., Jayakumar, D. A., Shailaja, M. S., and Narvekar, P. V., 2006. Seasonal oxygen deficiency over the western continental shelf of India*, in: Past and Present Water Column Anoxia*, edited by: Neretin, L. N., 195–224.

Parvathi, A., Jasna, V., Jina, S., Jayalakshmy, K. V., Lallu, K. R., Madhu, N. V., Muraleedharan, K. R., Naveen Kumar, K. R., Balachandran, K. K., et al. (2015). Effects of hydrography on the distribution of bacteria and virus in Cochin estuary, India. *Ecological Research, 30,* 85-92.

Pratihary, A. K., Naqvi, S. W. A., Narvenkar, G., Kurian, S., Naik, H., Naik, R., Manjunatha, B. R., 2014. Benthic mineralization and nutrient exchange over the inner continental shelf of western India. *Biogeosciences, 11*, 2771–2791, doi: 10.5194/bg-11-2771-2014.

Rajaneesh, K.M., Mitbavkar, S., Anil, A.C., Sawant, S.S., et al. (2015). Synechococcus as an indicator of trophic status in the Cochin backwaters, west coast of India. *Ecological Indicators, 55,* 118-130.

Revichandran, C., Srinivas, K., Muraleedharan, K. R., Rafeeq, M., Amaravayal, S. (2011). Environmental set-up and tidal propagation in a tropical estuary with dual connection to the sea (SW Coast of India). *Environmental Earth Sciences*, doi: 10.1007/s12665-011-1309-0

Shivaprasad, A., Vinita, J., Revichandran, C., Reny, P. D., et al. (2013a). Seasonal stratification and property distributions in a tropical estuary (Cochin estuary, west coast, India), *Hydrology Earth System Science, 17*, 187–199, doi: 10.5194/hess-17-187-2013.

Shivaprasad, A.; Vinita, J.; Revichandran, C.; Manoj, N.T.; Srinivas, K.; Reny, P.D.; Ashwini, R., and Muraleedharan, K.R., et al. (2013b). Influence of saltwater barrage on tides, salinity and chlorophyll-a in Cochin estuary, India. *Journal of Coastal Research*, *29*(6), 1382-1390, doi: 10.2112/JCOASTRES-D-12-00067.

Simpson, M.R. & Bland, R. (2000). Methods for Accurate Estimation of Net Discharge in a Tidal Channel. *IEEE Journal of Oceanic Engineering*, *25*(4), 437-445.

Sooria, P.M., Jyothibabu, R., Anjusha, A., Vineetha, G., Vinita, J., Lallu, K. R., Paul, M., Jagadeesan, L., et al. (2015). Plankton food web and its seasonal dynamics in a large monsoonal estuary (Cochin backwaters, India)-significance of mesohaline region. *Environment Monitoring Assessment,* 187-427.

Uncles, R.J. & Jordan, M.B. (1979). Residual fluxes of water and salt at two stations in the Severn Estuary. *Estuarine and Coastal Marine Science, 9*, 287-302.

Vinita, J., Shivaprasad, A., Revichandran, C., Manoj, N.T., et al. (2015a). Salinity Response to Seasonal Runoff in a Complex Estuarine System (Cochin Estuary, West Coast of India). *Journal of Coastal Research, 31*(4), 869-878, doi: 10.2112/JCOASTRES-D-13-00038.

Vinita, J., Shivaprasad, A., Manoj, N.T., Revichandran, C., Naveenkumar, K.R., Jineesh, V.K., et al. (in press). Spatial tidal asymmetry of Cochin estuary, West Coast, India. *Journal of Coastal Conservation: Planning and management.*

Vipindas, P. V., Anas, A., Jasmin, C., Lallu, K. R., Fausia, K. H., Balachandran, K. K., Muraleedharan, K. R., Nair, S., et al. (2015). Bacterial domination over Archaea in ammonia oxidation in a monsoon-driven tropical estuary. *Microbial Ecology*, *69*, 544-553, doi: 10.1007/s00248-014-0519-x.

Xavier, J. K., Joseph, T., Paimpillil, J. S., et al. (1993). Fluxes of Nitrogen in Chaliyar River Estuary, India. *International Journal of Ecology & Environmental Sciences, 31*, 223-229.

9. Legends

Figure 1. Map of Cochin estuary and Cochin inlet. Transect sampled across inlet using ADP and CTD sampling station is shown.

Figure 2. Monthly mean river runoff of Cochin estuary for the year 2010

Figure 3. Time series of physical parameters of neap (left panel) and spring (right panel) tides of dry season: (a&b) water level, (c&d) currents, and (e&f) salinity

Figure 4. Cross-channel current speed and direction contour plots showing maximum flood and ebb currents measured using ADP for neap and spring tides

Figure 5. Variations in water level and intra-tidal fluxes (m^3 s^{-1}) during (a) neap, (b) spring tides of dry season (Feb-Mar, 2010)

Figure 6. Nutrient distribution at Cochin inlet during neap and spring tides of dry season (Feb-Mar, 2010): (a) surface (b) bottom

Figure 1

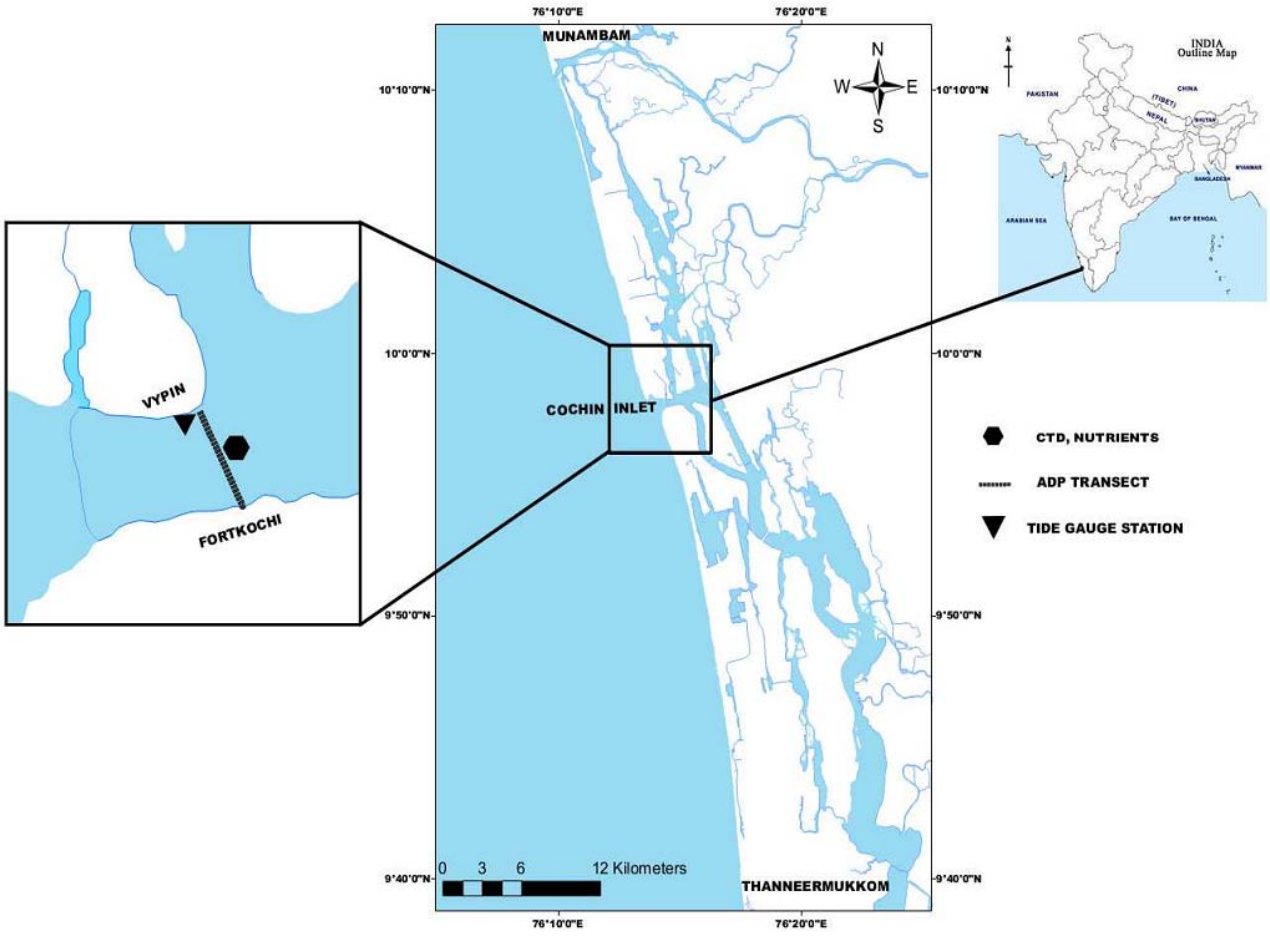
76°10'0"E
76°20'0"E
MUNAMBAM
10°10'0"N
N
W
E
S
INDIA
Outline Map
PAKISTAN
CHINA
(TIBET)
NEPAL
BHUTAN
MYANMAR
BANGLADESH
ARABIAN SEA
BAY OF BENGAL
VYPIN
FORTKOCHI
10°0'0"N
COCHIN INLET
CTD, NUTRIENTS
ADP TRANSECT
TIDE GAUGE STATION
9°50'0"N
0 3 6 12 Kilometers
9°40'0"N
THANNEERMUKKOM

Figure 2

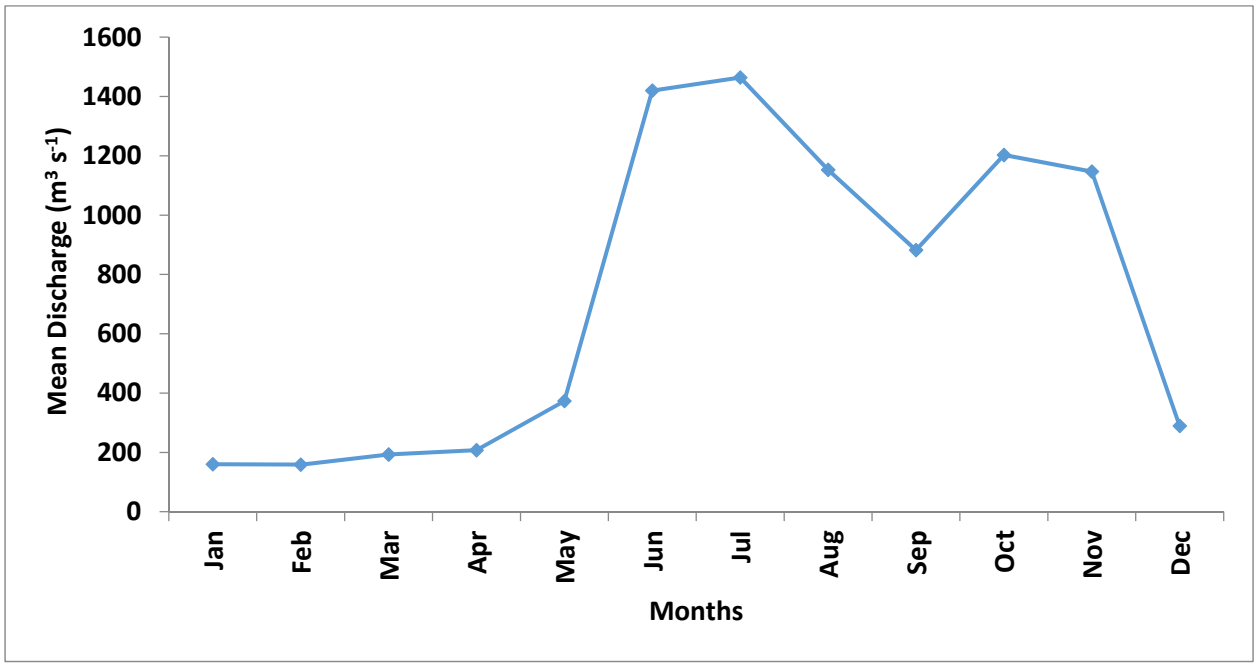
1600
1400
1200
1000
800
600
400
200
0
Mean Discharge (m³ s⁻¹)
Jan
Feb
Mar
Apr
May
Jun
Jul
Aug
Sep
Oct
Nov
Dec
Months

Figure 3

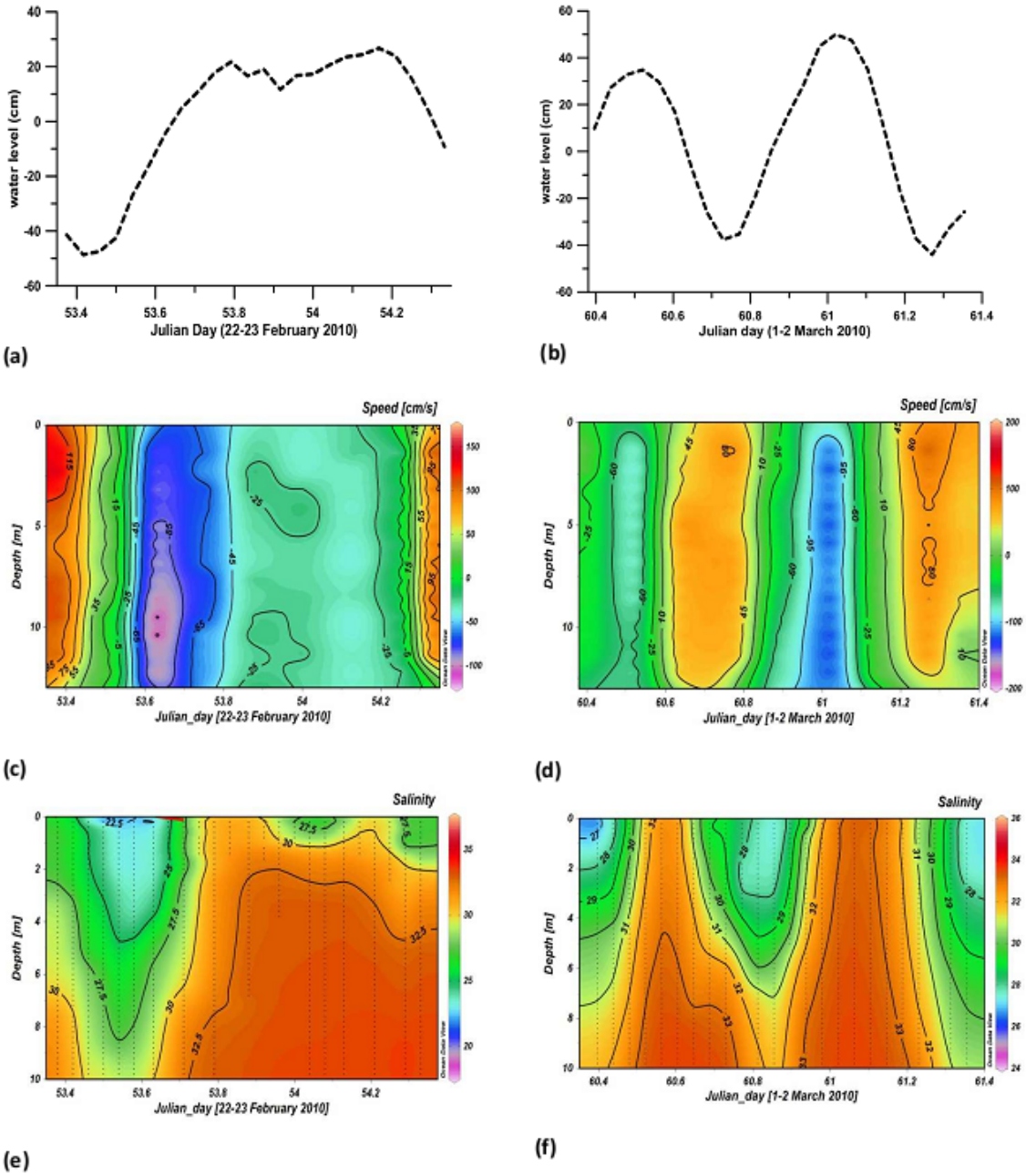
water level (cm)
Julian Day (22-23 February 2010)
(a)
water level (cm)
Julian day (1-2 March 2010)
(b)
Speed [cm/s]
Depth [m]
Julian_day [22-23 February 2010]
(c)
Speed [cm/s]
Depth [m]
Julian_day [1-2 March 2010]
(d)
Salinity
Depth [m]
Julian_day [22-23 February 2010]
(e)
Salinity
Depth [m]
Julian_day [1-2 March 2010]
(f)

Figure 4

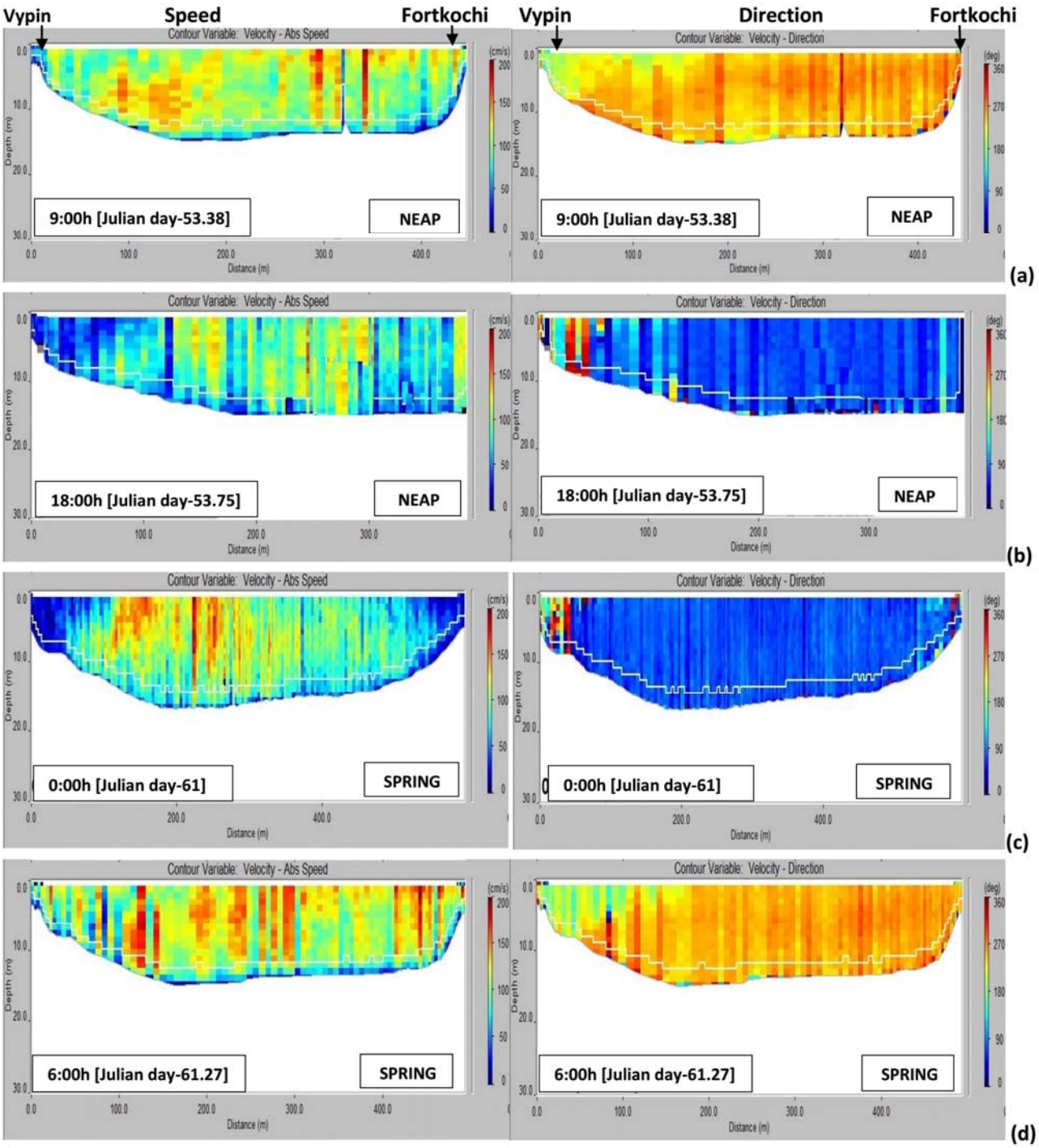
Vypin
Speed
Fortkochi
Vypin
Direction
Fortkochi
Contour Variable: Velocity - Abs Speed
Contour Variable: Velocity - Direction
Depth (m)
Distance (m)
(cm/s)
(deg)
9:00h [Julian day-53.38]
NEAP
(a)
18:00h [Julian day-53.75]
NEAP
(b)
0:00h [Julian day-61]
SPRING
(c)
6:00h [Julian day-61.27]
SPRING
(d)

Figure 5

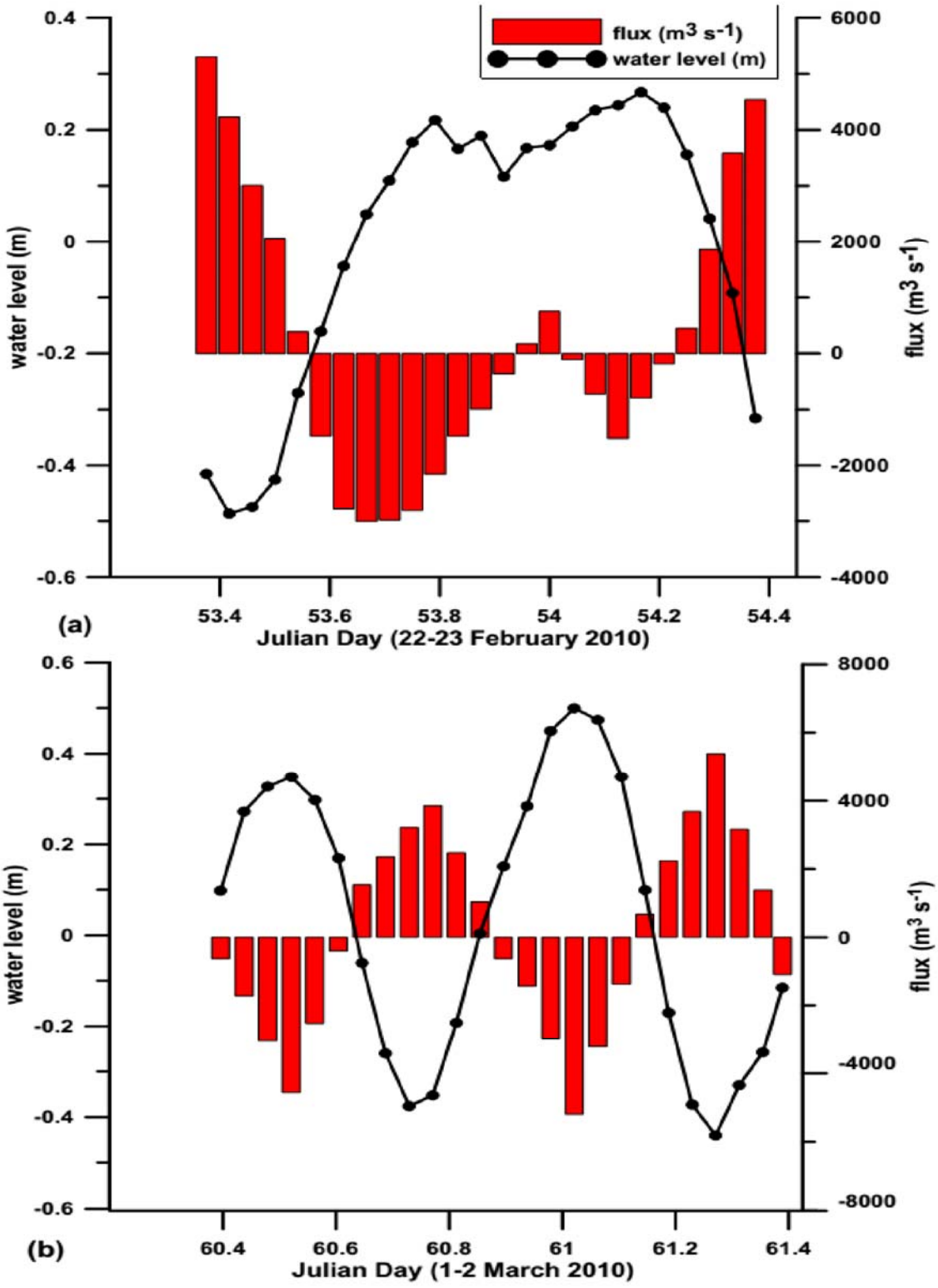
flux (m3 s-1)
water level (m)
water level (m)
flux (m3 s-1)
0.4
0.2
0
-0.2
-0.4
-0.6
6000
4000
2000
0
-2000
-4000
53.4
53.6
53.8
54
54.2
54.4
(a)
Julian Day (22-23 February 2010)
0.6
0.4
0.2
0
-0.2
-0.4
-0.6
8000
4000
0
-4000
-8000
60.4
60.6
60.8
61
61.2
61.4
(b)
Julian Day (1-2 March 2010)

Figure 6

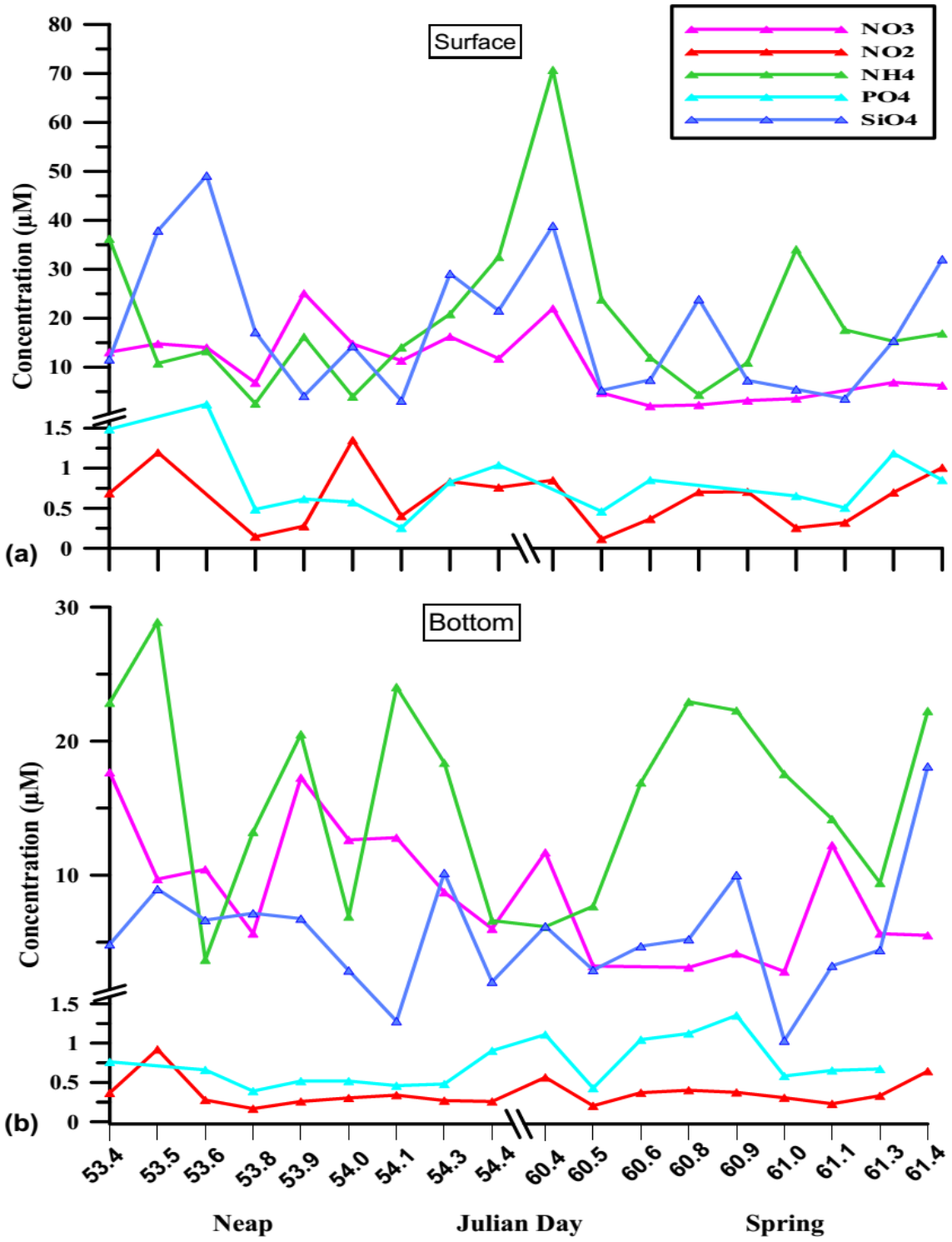
Surface
NO3
NO2
NH4
PO4
SiO4
Concentration (µM)
80
70
60
50
40
30
20
10
1.5
1
0.5
0
(a)
Bottom
Concentration (µM)
30
20
10
1.5
1
0.5
0
(b)
53.4
53.5
53.6
53.8
53.9
54.0
54.1
54.3
54.4
60.4
60.5
60.6
60.8
60.9
61.0
61.1
61.3
61.4
Neap
Julian Day
Spring

Table 1. Pearson correlation matrix for salinity and nutrients for dry season (a) Neap (b) Spring

(a) Neap

Variables	Salinity	NO3-N	NO2-N	NH4-N	PO4-P	SiO4
Salinity	**1**					
NO3-N	-0.175	**1**				
NO2-N	**-0.976****	0.213	**1**			
NH4-N	-0.122	0.213	0.093	**1**		
PO4-P	**-0.770***	0.057	**0.735***	0.297	**1**	
SiO4	**-0.837****	0.105	**0.770***	-0.018	**0.692***	**1**

(b) Spring

Variables	Salinity	NO3-N	NO2-N	NH4-N	PO4-P	SiO4
Salinity	**1**					
NO3-N	**- 0.614***	**1**				
NO2-N	**-0.888****	0.374	**1**			
NH4-N	-0.245	0.642	0.210	**1**		
PO4-P	**-0.700***	0.282	0.698*	0.252	**1**	
SiO4	**--0.772***	0.545	0.846**	0.527	0.678*	**1**

*: $P < 0.001$, **: $P < 0.0001$, bold values indicate negative correlation

Table 2. Material fluxes (t/d) of Cochin estuary in comparison with other systems in India

Location		NO3-N	NO2-N	NH4-N	DIN	DIP	SiO4-Si	Source
Hoogly estuary		-	-	-	180.27	35.07	117.26	Mukhopadyay et al. (2006)
Tapi estuary		-	-	-	-63.73	-17.3	-	Bapardekar et al. (2004)
Chaliyar estuary		-0.143	-0.02	-0.01	-0.17	-	-	Xavier et al. (1993)
Cochin estuary	Neap	81.13	4.88	245.68	331	20.06	108.07	Present study
	Spring	2.51	2.15	-132.9	-128.3	10.05	93.41	